a model to eliminate the adverse pressure gradient, the favorable pressure gradient was made less than that of a sphere cone. Intuitively, it would be expected that a reduction in the favorable pressure gradient would result in an increase in the disturbance growth rates and an earlier transition.

These present findings have some similarity to previous shock-tube transition results, which obtained transition data both within regions of favorable pressure gradients and downstream of the gradients.[5] It was found that transition on a hemisphere configuration first occurred near the sonic point. The supersonic portion of the hemisphere always had a laminar boundary layer until transition occurred near the sonic point; at which time, the entire supersonic region would experience transition, as if the boundary layer had been tripped. This result suggested that higher transition Reynolds numbers downstream of the sonic point might be obtained on a different configuration, such as an ellipse, which had the sonic point located closer to the stagnation point. Such a configuration would have a lower Reynolds number at the sonic point than a corresponding hemisphere at the same freestream conditions and perhaps delay the "tripping" of the supersonic boundary layer. Contrary to this reasoning, transition occurred at a lower Reynolds number in the supersonic boundary layer of the ellipse than on the corresponding hemisphere. Both the ellipse and hemisphere had cylindrical aft-bodies. When transition occurred on the cylindrical portion of both configurations, it was happening within a zero pressure gradient. The cylinder preceded by an ellipse always had a lower transition Reynolds number than the cylinder preceded by a hemisphere. It was speculated that the lower transition Reynolds numbers on the ellipse-cylinder configuration were associated with the weaker favorable pressure gradient downstream of the sonic point.

Another interesting comparison of these present results was found for situations in which transition was occurring closer to the nose tip (small X_T/X_{sw}). These data correspond to the smaller values of X_T/X_{sw} of Fig. 3, where Re_{x_T} steadily decreased to low values. Reference 3 discussed the sphere cone data, where this leg of the transition curve (called "early frustum transition") corresponded to situations in which a threshold value of Reynolds number at the sonic point was exceeded and the nose-tip conditions became the dominant parameters. This special model had a spherical nose tip that extended beyond the sonic point. Therefore, the subsonic flow and the sonic point conditions for this nose tip were similar to those for the sphere cone configuration with 10% bluntness ($R_N/R_B = 0.10$). For the 10% blunt sphere cone, it was not possible to exceed the nose-tip threshold conditions and obtain early frustum transition for any test conditions. Yet the threshold conditions for this present model were easily obtained, even with a smooth nose tip. These data in Fig. 3 correspond to the left branch of the data points, which extend parallel to the sphere cone early frustum transition data. These results indicated that the early frustum transition condition depended not only on nose-tip parameters but also on the subsequent pressure gradient. This appears to be another example of the importance of boundary-layer history.

References

[1]Stetson, K. F., "Effect of Bluntness and Angle of Attack on Boundary Layer Transition on Cones and Biconic Configurations," AIAA Paper 79-0269, Jan. 1979.

[2]Stetson, K. F., "Hypersonic Boundary Layer Transition Experiments," AFWAL-TR-80-3062, Oct. 1980.

[3]Stetson, K. F., "Nosetip Bluntness Effects on Cone Frustum Boundary Layer Transition in Hypersonic Flow," AIAA Paper 83-1763, July 1983.

[4]Fiore, A. W. and Law, C. H., "Aerodynamic Calibration of the Aerospace Research Laboratories $M=6$ High Reynolds Number Facility," ARL-TR-75-0028, Feb. 1975.

[5]Stetson, K. F., "Boundary Layer Transition on Blunt Bodies With Highly Cooled Boundary Layers," *Journal of the Aerospace Sciences*, Vol. 27, Feb. 1960, pp. 81-91.

Evidence of Reynolds Number Sensitivity in Supersonic Turbulent Shocklets

J. A. Johnson III,* Y. Zhang,† and L. E. Johnson‡
The City College, New York, New York

Introduction

THE existence of turbulent shocklets in supersonic free shear layers[1] affords new phenomena in these systems. Local shock waves can alter the transport of momentum from the free shear layer into the (surrounding) ambient environment and change the mixing processes at the boundary between the free shear layer and the ambient environment. This effect might explain the anomalous behavior in the spreading rate for supersonic free shear layers;[2] indeed some speculations have already been presented that model a local shock wave's induced negative vorticity as a cause of the reduced spreading rate.[3] A local shock wave can also destroy the evolution of supersonic combustion by rendering the local flow subsonic and thereby reducing the thrust which would otherwise be available in a scramjet.[4] In all of these discussions, it has been assumed that the shocklets are the direct consequence of the existence of turbulence in the free shear layer; it is also taken for granted that the control of the strength of the shocklets has a very high priority. In this Note, we report our first clear indication of a direct connection between these shocklets and turbulence. We will also show how this connection has implications for the prospect of shocklet control.

Experiments

Our tube wind tunnel is an elaboration of the configuration originally proposed by Ludwieg.[5] A conventional shock tube is modified by the insertion of a layer-spilling asymmetric supersonic nozzle into the section upstream from the diaphragm (the high-pressure section). When the diaphragm breaks, an expansion wave moves upstream into the high-pressure section through the nozzle causing the local pressure, density, and gas velocity to change with time and as a function of distance from the location of the diaphragm. At a time determined by the ratio of the nozzle's throat area to its exit area, the nozzle is choked, i.e., the mass flow rate is frozen, and stable, steady supersonic flow is established in the exit region. The duration of this steady period is determined by the round-trip time for the head of the expansion wave to travel from the throat of the nozzle to the upstream termination (end) of the high-pressure section. When the diaphragm breaks, other wave phenomena are also produced; viz, a shock wave and a contact surface travel downstream into the low-pressure section. In the literature, one can find derivations of the formulas relating the nozzle's parameters to the initial conditions of the tube.[6] With this kind of device, high Reynolds numbers (resulting from high stagnation pressures) can be maintained in the exit region under conditions of steady supersonic flow.

The low-pressure section of our Ludwieg tube has two parts: a 6-in.-diam, 5-ft long cylindrical end piece and a 3-ft-long transition piece that changes from 6-in.-diam circular cross section to a 3.6- × 3.6-in. square at the diaphragm. The transition piece has a hand-operated plunger for rupturing the diaphragm. The high pressure section has five parts: a 6-ft-

Received Feb. 17, 1987.

*Professor, Department of Physics. Member AIAA.

†Visiting Scholar, Department of Physics. (Permanent address: College of Science Management, Chinese Academy of Sciences, Beijing, People's Republic of China.)

‡Research Associate, Department of Physics.

long, 3.6- × 3.6-in. square test section with five optical ports on each face and corresponding pressure ports; a 3-ft-long transition piece for the change from a 3.6- × 3.6-in. cross section to the 6-in.-diam circle; a 5-ft-long, 6-in.-diam cylindrical piece; and two pieces that are each quarter-circle arcs of 2-ft radius with 6-in.-diam cross sections. The curved sections conveniently extend the overall length of the high-pressure section and thereby increase the duration of the period of steady supersonic flow. Wall thickness are roughly 0.3 in throughout.

Two rectangular nozzles have been built. Each one has an overall length of 28 in. with the nozzle's throat 9.5 in. from the upstream edge; in each case, one side has a wedge from the upstream edge to the throat joined smoothly to a second wedge from the throat to the exit while the other side has an upstream wedge to the throat and a flat extension of the throat to the exit. The nozzles are designed such that exit-to-throat area ratios produce Mach numbers of 1.6 and 2.0. Three kinds of diagnostics are used for the flow systems created by these nozzles: 1) wall-mounted quartz pressure gages throughout the test section whose outputs are recorded with oscilloscope cameras, 2) shadowgraph photography in the test section and 3) line-averaged slit shadowgraph photometry recorded through analog-to-digital encoding and offline computer analysis.

The starting processes in our facility are conventional and well understood.[7] The nozzles' freestream flow Mach numbers are calibrated directly by using wedges inserted in the flow and measuring the angles of the shock waves produced by the wedges. For each desired value of P_4 (the initial pressure in the high-pressure section), we determine the value of P_1 (the initial pressure in the low-pressure section) for which smooth (i.e., free of either expansion waves or shock waves) flow is achieved at the edge of the nozzle; this procedure defines the operating ratio P_4/P_1 for the given value of P_4 (and therefore the Reynolds number) at which measurements will be made. By thereby avoiding back pressure effects, we have created flow environments which can be generalized and are reproducible.

Results and Discussion

Turbulent free shear layers are produced in our Ludwieg tube which show turbulent shocklets. The shocklets that we see and the quantities that we measure are indicated schematically in Fig. 1. Specifically, we measure the angular rate of growth of the free shear layer and the turbulent shocklet's angle at large separation from the free shear layer (i.e., the Mach angle associated with the turbulent shocklet). Reynolds number (Re) variations come from changes in local freestream density (resulting from a change in the local operating pressure); local freestream velocity (resulting from a change in the Ludwieg tube's nozzle); and local charateristic length scale (also resulting from a change in the Ludwieg tube's nozzle and the resulting change in spreading rate). We have found that the spreading rate is determined entirely by the freestream Mach number and is independent of the local pressure. As Fig. 2 shows, the spreading rates for our free shear layers are quite consistent with those obtained at other laboratories. Figure 2 also shows that we have chosen nozzles with Mach numbers at the onset of anomalous spreading behaviors.[2]

The shocklet Mach angles show a sensitivity to changes in Reynolds number. This is summarized in Fig. 3. Overall, a 50% increase in Reynolds number produces roughly a 50% decrease in the shocklets' angles. The change in Reynolds numbers available is not yet adequate for us to distinguish the functional relationship clearly; nonetheless, our data suggest an unambiguous secular trend.

We can speculate that these shocklets are produced by some entity imbedded in the flow moving at a speed different from that of the local gas. Therefore, the change in θ implies a change in the turbulent shocklet-producing entity's velocity with respect to the local flow. We can represent this velocity as v_{se}, where $M_{se} = (\sin \sigma)^{-1}$, $v_{se} = M_{se}a_e$ and a_e is the local speed of sound in the supersonic freestream. The local laboratory velocity is approximately given by $v_{lse} = V - v_{se}$ where V is the local (supersonic) velocity in the freestream. Figure 3 gives M_{se} vs Re. Since the shocklet's Mach angle is a measure of the strength of the shock wave,[8] Fig. 3 suggests that the increasing Reynolds numbers cause increasing strengths in the shocklets produced by the turbulence. Since the profile of a shadowgraph's signal is well known, we have used dual-beam continuous shadowgraph photometry as a detector of shock waves and calibration for the velocity measurements. Specifically, two sensors, separated by 0.4 cm parallel to the supersonic stream colinear with the surface of the nozzle and 1.8 cm

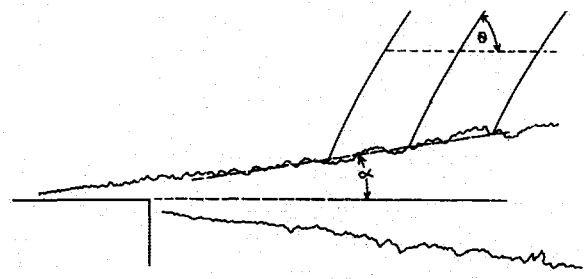

Fig. 1 Schematic of turbulent shocklets. The free shear layer spills off the edge of the nozzle. The dashed lines indicate reference lines for the two angles which we measure (directly from the shadowgraph photographs): α is the half-angular rate of growth of the shear layer; θ is the Mach angle associated with the turbulent shocklet.

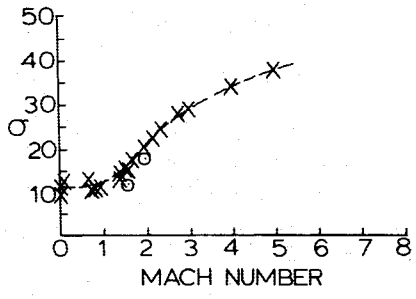

Fig. 2 Spreading rate vs Mach number for free shear layers. The units for σ are rad^{-1}. The X's are data from Ref. 2; the dashed line is an approximate smooth curve through the X's. The two circles are our measurements with $\sigma = \frac{1}{2}\alpha$: at Mach number $M = 1.6 \pm 0.1$ we found $\sigma_{1.6} = 11 \pm 1$ rad^{-1}; at $M = 2.04 \pm 0.04$ we found $\sigma_{2.0} = 17 \pm 2$ rad^{-1}.

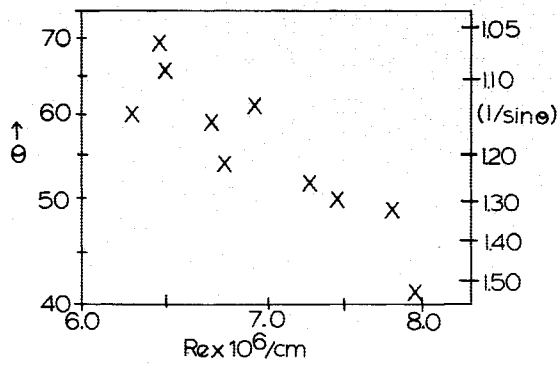

Fig. 3 Turbulent shocklet mach angle vs Reynolds number. The Reynolds number (Re) was computed as $Re_i/\text{cm} = \rho V \alpha_i / \mu \alpha_{1.6}$ where: the length scale is normalized to the scale at $M = 1.6$ using $\alpha_{1.6}$ the half-angular spreading rate at $M = 1.6$; V is the measured freestream velocity; μ and ρ are the freestream viscosity and density computed using the measured parameters; and α_i is the half-angular spreading rate at Mach number M_i. The axis on the right side shows $M_{se} = (1/\sin\theta)$, which is the apparent Mach number of the shocklet-producing entity.

from the edge, provide evidence of the movement of a local shock wave through the free shear layer. The velocity measurements now available from these observations have an uncertainty of at least 20%; however, they are quite consistent with velocity measurements from the shocklets' Mach angles.

From these results, we can speculate that a functional relationship exists between the strength of a turbulent shocklet and Reynolds number. We know that, in the early stages of turbulence, there is a confirmed relationship between turbulent intensity and Reynolds number;[9] our observations may be hostage to this relationship. However, the relationship between turbulent intensity and Reynolds number has a characteristic frequency as its control parameter. Therefore, an adjustment in the characteristic frequency can change the nature of this relationship and, in turn, change the strength of the shocklets. The Reynolds number is also altered, of course, by changes in characteristic length and in viscosity and local velocity; this means that direct variation in Reynolds numbers, even at fixed flow velocity, can cause a direct variation in the strength of the shocklets. Since there is an apparent influence of Reynolds number on the strength of the shocklets, the options cited allow us to anticipate the control of turbulent intensity as an avenue for the control of the supersonic mixing.

Conclusions

The systems of internal shock waves produced in turbulent free shear layers are correlated with Reynolds number. This correlation implies a direct connection with turbulent intensity. Through this connection and the adjustability of the Reynolds number, some opportunities may be found for the control of turbulent shocklets and thereby the control of their influence on supersonic mixing.

Acknowledgment

This work was supported in part by NASA Grant NAG-1-377.

References

[1]Oertel, H., "Kinematik der Machwellen innerhalb und ausserhalb von Uberschallstrahlen," ISL-R 112/78 (1978); also, Oertel, H., "Machwave Radiation of Hot Supersonic Jets Investigated by Means of the Shock Tube and New Optical Techniques," *Shock Tubes and Waves; Proceedings of the 12th International Symposium on Shock Tubes and Waves,* edited by A. Lifshitz and J. Rom, Magnum Press, Jerusalem, Israel, 1980, pp. 266-275.

[2]Morrisette, E. L. and Birch, S. F., "Mean Flow and Turbulence Measurements in a Mach 5 Shear Layer, Part I—The Development and Spreading of the Mean Flow," *Fluid Mechanics of Mixing,* ASME, New York, 1973, pp. 79-81; also Anon, "Free Turbulent Shear Flows," Vol. I—Conference Proceedings, NASA SP-321, 1973.

[3]Zang, T. A., Hussaini, M. Y., and Bushnell, D. M., "Numerical Computations of Turbulence Amplification in Shock-Wave Interactions," *AIAA Journal,* Vol. 22, Jan. 1984, pp. 13-21.

[4]Strehlow, R. A., *Combustion Fundamentals,* McGraw-Hill, New York, 1984, pp. 331-332.

[5]Ludwieg, H., "Der Rohrwindkanal," *Zeitschrift fur Flugwissenschaft,* Jahrgang 3, Heft 7, July 1955, pp. 206-216; also H. Ludwieg, "Tube Wind Tunnel: A Special Type of Blow Down Tunnel," NATO Headquarters, Scheveningen, Holland, AGARD Rept. 143, June 1952.

[6]Cable, A. J. and Cox, R. N., "The Ludwieg Pressure-Tube Supersonic Wind Tunnel," *The Aeronautical Quarterly,* Vol. XIV, Pt. 2, May 1983, pp. 143-157.

[7]Johnson, J. A., III and Cagliostro, D., "Startling Phenomena in a Supersonic Tube Wind Tunnel," *AIAA Journal,* Vol. 9, Jan. 1971, pp. 101-105.

[8]John, J. E. A., *Gas Dynamics,* Allyn and Bacon, Boston, MA, 1969, pp. 274-275.

[9]Osborne, M. R., "Numerical Methods for Hydrodynamic Stability Problems," *SIAM Journal of Applied Mathematics,* Vol. 15, No. 3, 1967, pp. 539-557.

Optimum Synthesis of Polymer Matrix Composites for Improved Internal Material Damping Characteristics

P. Hajela* and C.-J. Shih†
University of Florida, Gainesville, Florida

Introduction

THE present paper examines the optimum internal material damping characteristics of short-fiber, polymer matrix composites. Internal damping depends the properties of the fiber and matrix materials and on the geometrical layout of the composite. Damping properties of continuous and short-fiber composites have been studied and documented in the literature.[1] Glass- and graphite-reinforced polymer matrix composites exhibit anisotropic, linear viscoelastic behavior, and the principal mechanism of damping in such composites is considered to be the viscoelastic energy dissipation in the matrix material. Stress concentration effects in discontinuous fiber composites facilitate the transfer and dissipation of energy in the viscoelastic polymer matrix and, therefore, yield a higher level of internal damping.

The elastic-viscoelastic correspondence principle has been used in conjunction with a force-balance approach to obtain analytical estimates of internal damping in short-fiber composites.[2] This approach essentially develops relations for the loss and storage modulii of the composite in terms of the fiber aspect ratio, loading angle, stiffness of fiber and matrix materials, the fiber volume fraction, and the damping properties of the fiber and matrix materials. The present paper proposes a design synthesis procedure based on formal multidimensional optimization in which the extensional loss factor of a representative volume element is maximized, subject to constraints on the element mass and stiffness characteristics. Two distinct analysis models, one that uses Cox's shear-lag theory,[3] and another based on an advanced shear-lag theory that allows for the matrix to partially sustain extensional loads,[4] are used in the present work. These analytical models and their adaptation in optimum synthesis are discussed next.

Analysis and Optimum Synthesis Problem

A representative volume element, shown in Fig. 1, describes the geometrical relationship between the fiber and matrix materials. Short fibers of length s and diameter d are embedded in a matrix element of length $s+p$ and diameter D. The ratio s/d is referred to as the fiber aspect ratio and p/s denotes the discontinuity ratio. The extensional modulus in the x direction is written as a complex quantity

$$E_x^* = E_x' + iE_x'' \tag{1}$$

where E_x' and E_x'' are the storage and loss modulii, respectively; the ratio $\eta_x = E_x''/E_x'$ is the loss factor and a measure of the internal damping. The expression for E_x^* is obtained in terms of longitudinal modulus E_L^*, transverse modulus E_T^*, shear modulus G_{LT}^*, and Poisson's ratio ν_{LT}, where the transverse and shear modulii are obtained by the use of the Halpin-Tsai equations and the rule of mixtures. The longitudinal modulus is derived from the force equilibrium of the compos-

Received Feb. 10, 1987; presented as Paper 87-0865 at the 28th AIAA/ASME/ASCE/AHS Structures, Structural Dynamics and Materials Conference, Monterey, CA, April 6-8, 1987; revision received Aug. 21, 1987.

*Associate Professor, Department of Engineering Sciences. Member AIAA.

†Graduate Assistant. Student Member AIAA.